MR. GIACOMO POCCI, *Chief of the Research Bureau*

Ministry of Transportation

INTRODUCTION

Good morning ladies and gentlemen. It is my pleasure to introduce the Italian technical presentations which will consist of first, Engineer Moscarini, Director of the Experimental Institute for Motor Vehicles (ISAM) who will report on a technical paper titled "Vibrations Influencing Driver's Fatigue." Mr. Moscarini will then be followed by the Alfa Romeo presentations by Dr. Cacciabue on "Passive Restraints" and Dr. Schiappati on "Active Restraints." Finally, Dr. Montabone will introduce the technical presentation by the Fiat S.P.A., Mr. Moscarini . . .

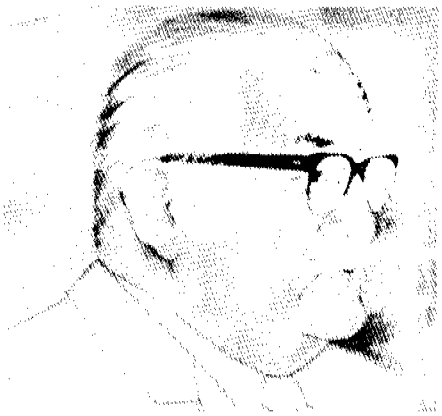

ITALY

DR. FLAVIANO MOSCARINI, *Director*

Experimental Institute for Motor Vehicles

ISAM, Istituto Sperimentale Auto e Motori, is a scientific organization involved in applied research.

ISAM is a member of the Italian working group concerned with studies to solve the problem of vehicle safety for the Italian Ministry of Transportation.

Most authorities agree that drivers are responsible for about 90% of all accidents. Recognizing this fact, one understands the real role played by human factors in accident cases. Human factors, therefore, have to be taken into account in any safety vehicle concept.

ISAM activity is also involved in human engineering. The first item is intended to define new standards for acceptable vehicle driving characteristics. The second subject is concerned with research on driver environment conditions in the car, especially from the viewpoint of effects on the driver's reaction. This subject may be divided in two different parts: first, the design of really psychological seats easily adaptable to a wide range of people, and second, research on vibrations transmitted by the car to the driver. These vibrations cover a wide frequency range from ultrasound to infrasound and their effects have to be accurately investigated. The difficulties in accomplishing this research arise because suitable instruments are not available as noted by authorities such as Bryan, Tempest and Mohr.

We are working in vibration research field in cooperation with the Department of Sport Medicine of the University of Rome, and we hope to have in the near future some interesting results on the effects of vibrations on man. To conduct these investigations, we have almost completed a vibrating platform on which a seat may be mounted and then excited at different vibration frequencies. We are also planning the design of a system able to apply contemporarily different vibratory waves to the platform. In this manner we will also be able to investigate the effects of a random vibration pattern. The platform design allows us to study vibration effects on human vision through the wind-screen, both inclined and curved. It allows us, at last, to study modifications of human eye capability due to effects of vibrations and sounds.

FRONTAL CRASH – INFLUENCE OF THE DECELERATION MODE (AT THE SEAT BELTS ANCHORAGE POINTS) ON SEVERITY INDICES

DR. ANTONIO CACCIABUE *Expert,*
Motor Vehicles Safety Design Office

INTRODUCTION

The purpose of restraining devices for vehicle occupants is that of ensuring, during the crash, their connection to a practically undeformable part of the vehicle in such a way that the deceleration mode of the dummy is as uniform as possible, and its level as low as compatible with the crash conditions and the available "ride down" distance. An ideal occupant restraint system should be able to ensure the above mentioned conditions for all the vital parts of the body, which must be considered as a system with many degrees of freedom, and a certain number of masses interlinked by means of free and relatively weak hinges, through which only comparatively modest forces can be transmitted.

In order to approach as much as possible such an ideal, actual restraining devices are generally made up of a few components, which reciprocally interact. More specifically, a safety belt (the component we intend to examine here) has the job of restraining the central part of the body directly, and only indirectly the extremities, such as head and legs, according to whether there are other, complementary restraining systems. As we have already mentioned, a satisfactory study of the stresses imposed on the body during a frontal crash, especially on those parts not directly restrained by the belt, involve a several degree of freedom approach, taking into account the complex contour conditions. Such simulations, which are now widespread, can give interesting overall indications; but due to the great number of variables involved, do not appear suitable to emphasize efficiently the influence of safety belts characteristics and of the deceleration modes of their anchorages on the dummy's motion.

To this end we believe quite useful a simple scheme limited to the central part of the body, which is assumed to be a concentrated mass, connected to the vehicle by means of a belt with given deformation characteristics. The law of motion of the belt anchorages is also assumed known.

We would again like to stress that such a simplified scheme cannot give reliable results for the whole dummy, even if we consider it quite suitable for the present purpose.

The Severity Indices thus obtained are only indicative values, and serve for comparison between different belt solutions, and deceleration modes.

MATHEMATICAL TREATMENT

From Figure 1 we obtain the scheme used afterwards for the discussion of Figure 2.

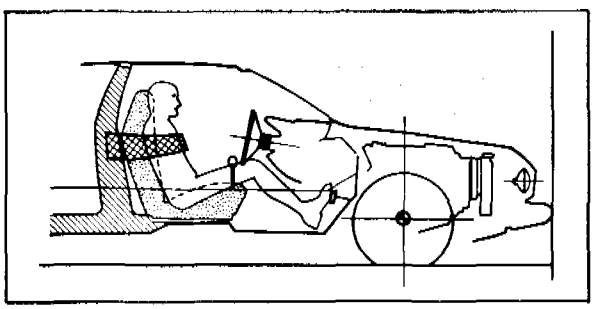

FIGURE 1

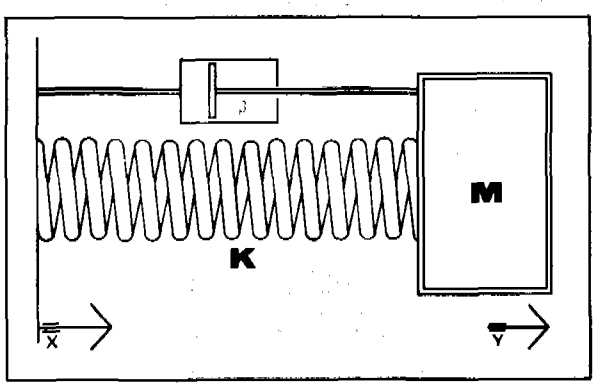

FIGURE 2

We have:

x = total displacement

x = total displacement of the belt anchorage point during the crash.

y = total displacement of the mass restrained by the belt during the crash.

at time t = 0, x = 0 and y = 0.

k = elastic rigidity of the belt.

β = viscous damping coefficient of the belt.

Assuming a displacement law for x, then the motion of y can be studied, for given values of belt elasticity and damping coefficent.

Anchorage displacement law

Figure 3 shows an experimental diagram (obtained from actual crash test results of one of our production cars) for the deceleration of a point on the body, which may be considered a belt anchorage. This diagram shows also the velocity and displacement curves. From this it can be seen that for a 30.95 mph crash the anchorage point displacement is L = 0.65 m.

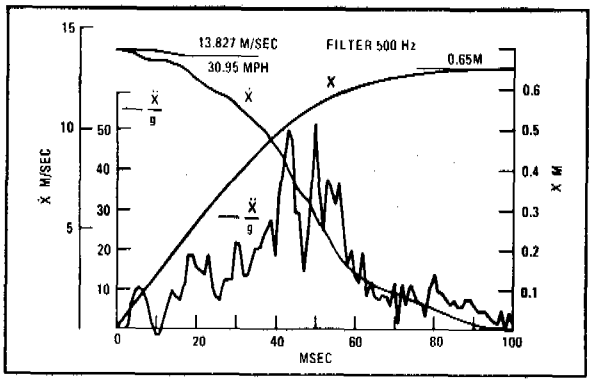

FIGURE 3

Occupant mass and elastic characterisitics of the belt

In the following calculations a mass of 65.7 Kg was considered, assuming that part of the body mass, indirectly restrained by the belt, would be restrained by other complementary systems. The belt is characterized by a constant rigidity k, and by a viscous damping coefficient β. This assumption approximates quite closely to the actual behavior of existing safety belts. Two cases were examined:

- Conventional "elastic" belts, characterized by low damping. The assumptions were:

$$k = 10000 \text{ Kg/m}$$
$$\beta = 0.5\ \beta_{cr} = \sqrt{km} = 258.6\ \frac{\text{Kg. sec.}}{\text{m}}$$

- Critical damping belts.
To enable us to compare the results of this belt with the one above, it was decided to assume a value for k and for the corresponding damping coefficent $\beta cr = 2\sqrt{km}$, such that the maximum elongation obtained was the same as the one with the "elastic" belt.

Procedure for comparing the two belts.

The comparison was done by studying the law of motion of the mass m for each type of belt, and assuming the following Severity Indices (with respect to the anchorage points and the mass of the dummy) as a comparison yard-stick:

$$SIX = \int_0^t \left(\frac{|\ddot{x}|}{g} \right)^{2.5} dt$$

$$SIY = \int_0^t \left(\frac{|\ddot{y}|}{g} \right)^{2.5} dt$$

To evaluate the SIX, the integral was taken over the whole duration of the crash (100 msec.) For SIY, instead, the integral was taken only up to the point where $\ddot{y}$ changes sign.

ANALYSIS OF THE RESULTS OBTAINED

Figures 4 and 5 show the diagrams of decleration, Severity Indices, velocity and displacement of the anchorage points and of the mass m, for both types of belts considered. In the following table we have shown the Severity Indices obtained, and also their ratio.

k Kg/m	β/β_{cr}	Max. Elongation m	SIX	SIY	SIY/SIX
10000	0.5	0.150	186	190	1.022
5500	1	0.150	186	144	0.774

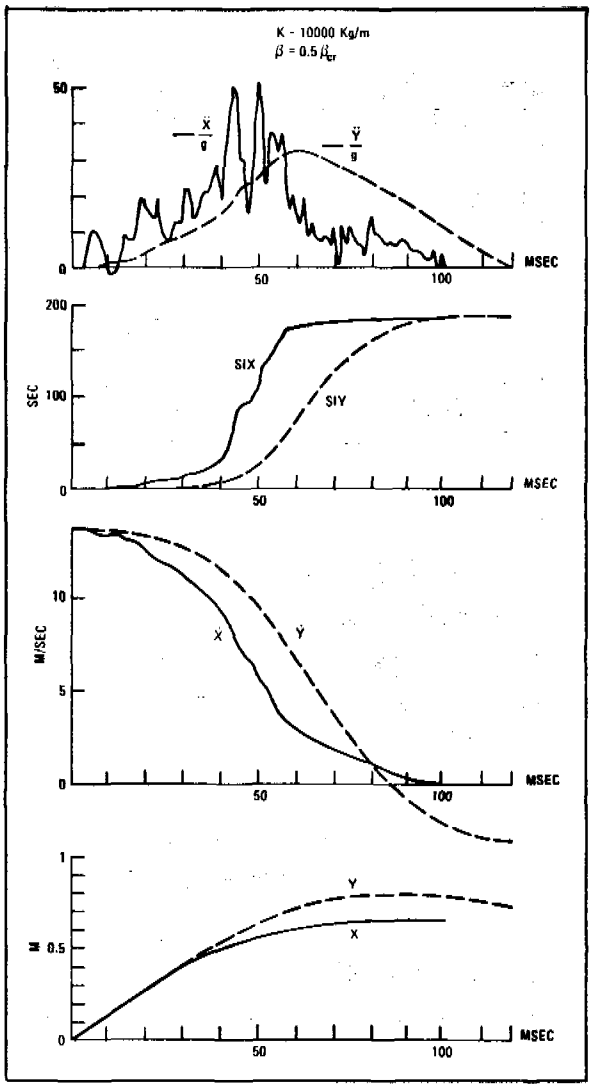

FIGURE 4

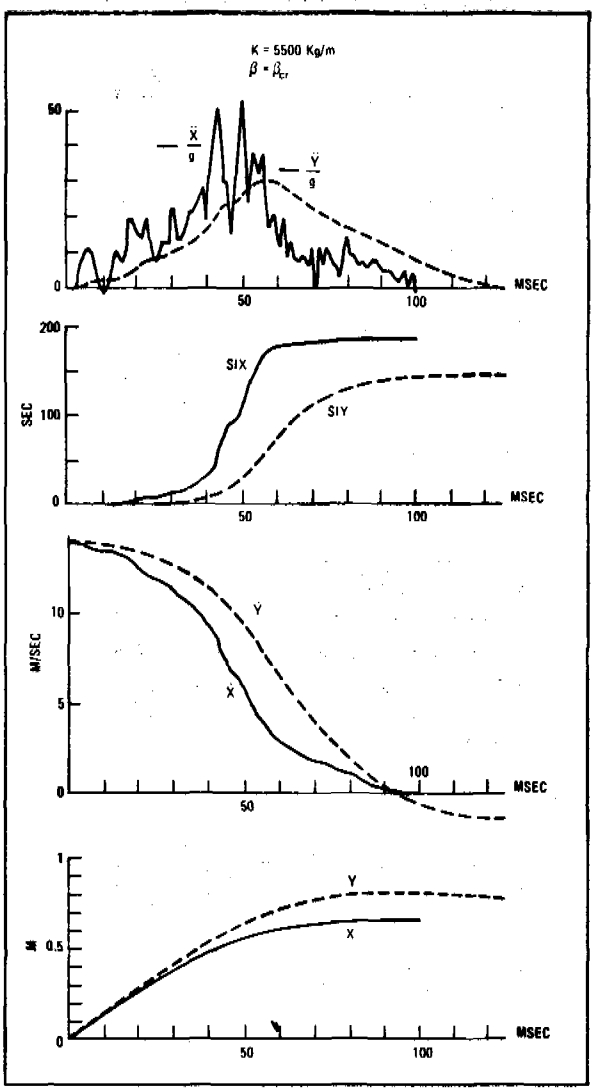

FIGURE 5

We can observe the following points:

- The Severity Index for the mass m obtained with the critical damping belt is lower than the one obtained with the conventional belt.
  The better behavior of the former belt was found also using anchorage deceleration diagrams widely differing from the one used in the above mentioned calculation.
- For both types of belts, it was noted that the Severity Indices calculated for the mass m and for the anchorage points did not vary greatly.

It would be possible to obtain significantly lower values for the Severity Indices using "constant force" belts, which would give a close approximation to the ideal of a rectangular deceleration diagram for the mass m.

In this case we would have:

$$(SIY)_{id} = \frac{u^4}{[2(L+\Delta L)]^{1.5}\, g^{2.5}} = 59.9$$

where:

u = crash velocity = 13.827 m/sec.

$L+\Delta L$ = total mass displacement = 0.65 + 0.15 = 0.8 m.

- The contour of the mass deceleration diagrams, for both belts, is smoother than the corresponding one for the anchorage points.

RESEARCH ON THE BELT FILTERING EFFECT

The experimental diagram shown in Figure 3 was developed using Fourier series (with a base of 100 msec.), in order to establish the importance of the belt filtering effect on the Severity Index of the mass m. This development was carried out up to the tenth harmonic. Using both belts under consideration, a series of calculations was performed, with anchorage deceleration diagrams built up starting with the constant component of the development, and successively adding the various harmonics, up to the tenth.

Figures 6 and 7 show the diagrams corresponding to the first 3 deceleration laws.

In the following table, and in the diagram of Figure 8, we have shown the values of SIX, SIY and SIY/SIX for excitation diagrams drawn with the successive addition of harmonics up to the tenth. It can be seen that the filtering effect of both types of belts is such that the contribution of those harmonics higher than the first to the Severity Index is practically nil.

FIGURE 6

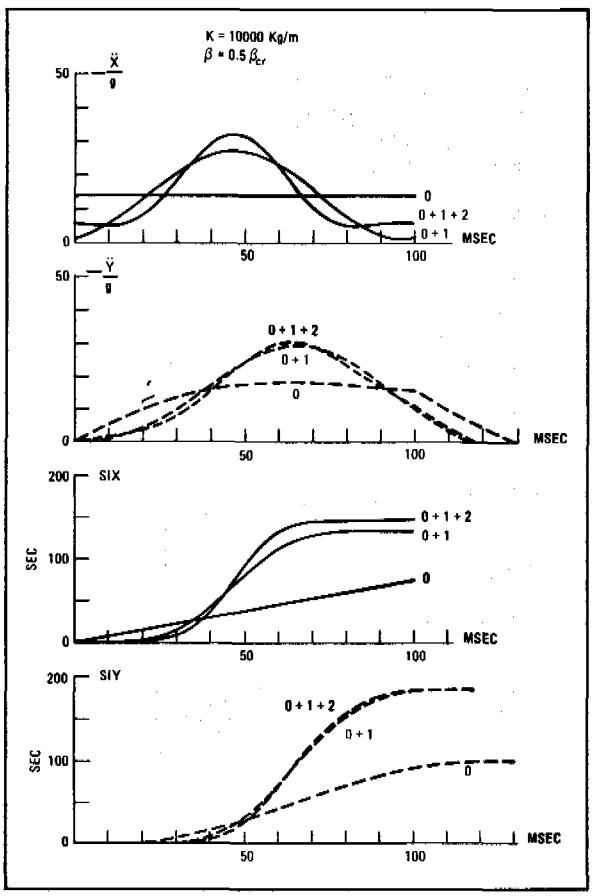

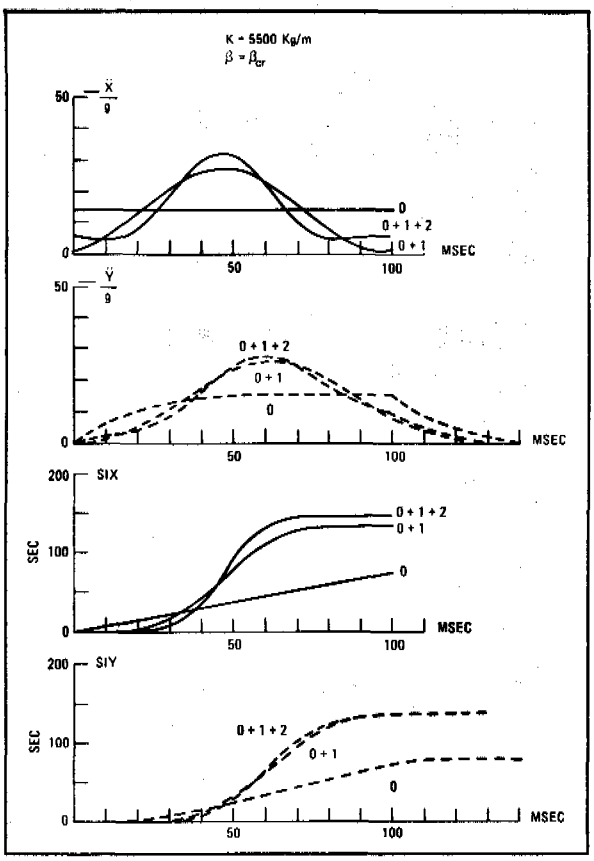

FIGURE 7

Σ Harmonics	SIX	SIY $\beta = 0.5\beta_{cr}$	SIY $\beta = \beta_{cr}$	SIY/SIX $\beta = 0.5\beta_{cr}$	SIY/SIX $\beta = \beta_{cr}$
0	75.	100.	81.	1.33	1.08
0 ÷ 1	134.	186.	140.	1.39	1.04
0 ÷ 2	148.	185.	141.	1.25	0.95
0 ÷ 3	158.	187.	142.	1.18	0.89
0 ÷ 4	159.	187.	142.	1.18	0.89
0 ÷ 5	159.	187.	142.	1.18	0.89
0 ÷ 6	160.	187.	142.	1.17	0.89
0 ÷ 7	160.	187.	142.	1.17	0.89
0 ÷ 8	163.	187.	142.	1.15	0.87
0 ÷ 9	165.	187.	142.	1.13	0.86
0 ÷ 10	166.	187.	142.	1.13	0.86
...					
0 ÷ ∞	186.	190.	144.	1.02	0.77

CONCLUSIONS

The traditional, elastic type belts examined gave similar Severity Indices for the mass and for the anchorages. Some improvement could be obtained

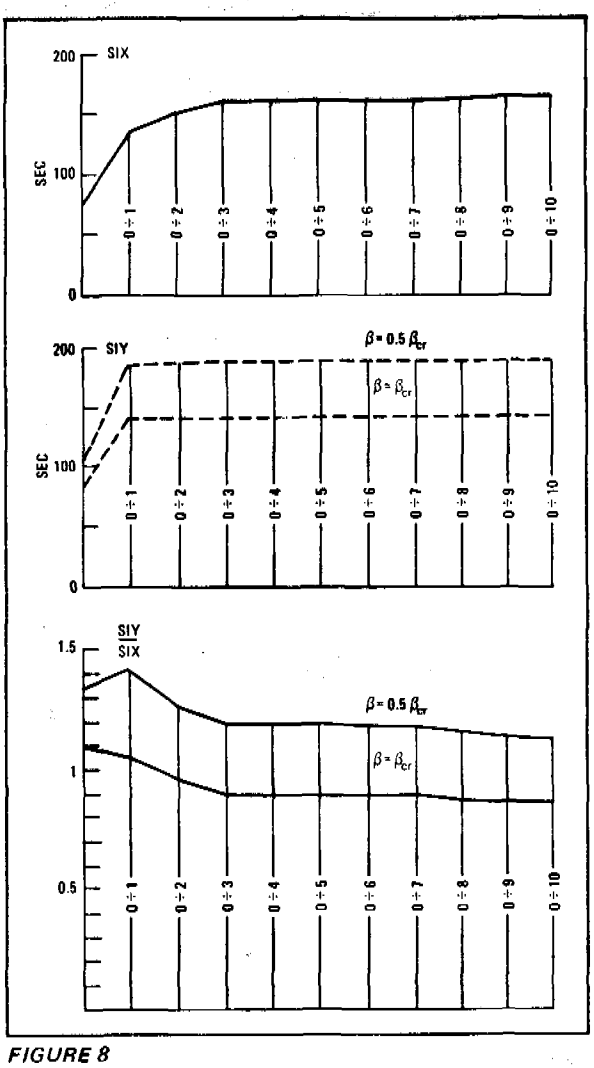

FIGURE 8

with critical damping belts. Much better results could be given by constant force belts.

It must be pointed out, however, that the Severity Indices calculated were relatively low.

The filtering system, consisting of the body mass (assuming attached to the free end of the belt) and of the elastic rigidity of the belt, renders the mass rather unsensitive to the shape of the deceleration diagram attributed to the anchorages. More particularly, only the first harmonic of the Fourier series development of the excitation diagram can make a noticeable difference to the Severity Index of the mass restrained by the belt. This is mainly due to the low frequencies inherent in the mass–belt system, which are (for $\beta = 0$):

$K = 10000$ Kg/m $f = 6.15$ Hz
$K = 5500$ Kg/m $f = 4.56$ Hz

while the lowest frequency of the exciting system is 10 Hz, for an impact duration of 100 msec.

The experimental deceleration diagrams for the anchorage points may be considered indicative of the stress imposed on the occupants, only if the higher order harmonics (which do not modify the phenomenon) are neglected.

From the results obtained, it seems logical to give rather little importance to the shape of the deceleration diagrams of that part of the body structure which remains practically undeformed, and especially to the belt anchorage points. It is quite sufficient if the deceleration diagram has a "compact" area for the time interval in which vehicle deformation takes place, while even the high "peaks" of decelerations have negligible effect on the occupants Severity Indices. Hence it is better to attribute much more importance to the usable "ride down" distance, considered as the sum of the vehicle deformation and the maximum belt elongation allowed by the size of the interior and its deformation.

We believe that this distance could be usefully increased without revolutionizing the architecture of present-day vehicles, and without substantial cost, weight, size and performance penalties. For example, noticeable advantages could be obtained by adopting short engines, and reducing the rearward movement of the steering wheel, below the limit imposed by the present legislation. Other possibilities to be considered are bumpers which extend as the vehicle speed increases.

For the vehicle energy absorbing structure, having noted that the obtainment of a deceleration law similar to the ideal one is not essential, the purpose of studies and research must become:

- The obtainment of the optimum amount of deformation of the structure with an acceptable deceleration law. This optimum is, obviously, the one which provides the greatest distance for the occupants to decelerate.
- The achievement of the lowest possible weight.

In the light of this, the difficulties of structural studies become less severe: a structure, which has not been optimized for stress and deformation distribution during the impact, will show a weight penalty, but not necessarily worse occupants Severity Indices. It must be remembered, of course, that the above-mentioned weight penalty has important effects on cost and road-holding.

ACTIVE SAFETY. A CONTRIBUTION TO THE STUDY OF THE VEHICLE-DRIVER SYSTEM. A FIRST APPROACH TO THE DEFINITION OF AN UNDULATION SURFACE FOR ROAD-HOLDING TESTS.

DR. ING. ANGELO SCHIAPPATI
Alfa Romeo Technical Staff

INTRODUCTION

At the Second International ESV Conference in Germany, we talked about Alfa Romeo's opinion on Active Safety. More particularly, we showed the phases which experimental and theoretical research undergo:

- An experimental study of the vehicle-driver system, as knowledge in this field is still insufficent. This was shown, amongst other things, by the doubts and criticism on the American ESV requirements on active safety observed during the Stuttgart conference.
- Interpretation and generalization of the experimental study using sufficiently reliable mathematical models. Actually, it is practically impossible to carry out completely satisfactory tests which will allow a clear understanding of each of the most important dynamic parameters of vehicle motion. This is mainly due to the variation in the behavior of different drivers and, even for the same driver, the variation with respect to time. It is instead possible to estimate, from experimental data, a standard driver behavior, and hence evaluate the influence of those parameters related to vehicle motion, by using an appropriate mathematical model.
- The obtainment of dynamic parameters for the optimization of the vehicle and of the acceptable limits for the variation of real parameters from the optimum configuration.
- A study of objective experimental tests to establish if the vehicle dynamic behavior falls within acceptable limits.

In what follows we show some of the results obtained from research on the driver-vehicle system (points a, b, c) and on experimental tests (point d).

DRIVER-VEHICLE SYSTEM RESEARCH

A series of experiments (which is still continuing today) was carried out on our vehicles, with different drivers and maneuvers. Most of this work was done on the following two maneuvers:

- Entry to and exit from a circular arc bend joining two perpendicular straight lanes.
- Change of trajectory on a straight road, simulating a lane changing maneuver to overtake, or to avoid an obstacle which was noticed rather late by the driver (for instance, a queue of stationary vehicles).

Having established the dynamic characteristics of the vehicle, the experimental results were utilized to define the driver behavior using two parameters, according to the mathematical model we showed at Stuttgart last year. In other words, the driver's reaction time and the parameter for the accuracy of the extrapolation estimate were obtained through a regression analysis performed on a certain number of vehicles and drivers, neglecting evaluations on either particularly good or bad drivers.

Hence, considering the driver's characteristic parameters constant and starting from a configuration typical of one of our production vehicles with good road-holding, a study on the effects of varying a great number of dynamic parameters of the vehicle was carried out. Below we show some of the more interesting results thus obtained, pertaining to the straight road lane-changing manoeuvre. More particularly, we will discuss the influence of some of the parameters chosen from the ones most susceptible to variations, especially considering the structural modifications envisaged to conform to possible future passive safety requirements.

Vehicle characteristics

Case 0 – Base vehicle.

total mass of the vehicle (60% of maximum load)	137.5 Kgsec^2/m
sprung mass	120.3 Kgsec^2/m
wheelbase	2.57 m
distance of the vehicle center of gravity from the front axle	1.235 m
distance of the vehicle center of gravity from the rear axle	1.335 m
front track	1.32 m
rear track	1.27 m
height of the center of gravity of the vehicle	0.5 m
distance of the center of gravity of the sprung mass from the roll axis	0.33 m
front roll center height	0.02 m
rear roll center height	0.38 m
front unsprung mass	7.14 Kg sec^2/m
rear unsprung mass	10.20 Kg sec^2/m
height of the center of gravity of the front unsprung mass	0.286 m
height of the center of gravity of the rear unsprung mass	0.286 m
vehicle moment of inertia about the yaw axis	202.4 Kgmsec^2
moment of inertia of the sprung mass about the roll axis	52.05 Kgmsec^2
product of inertia of the sprung mass for yaw and roll axes	25.59 Kgmsec^2
front roll stiffness	2524. Kgm/rad
rear roll stiffness	908. Kgm/rad
front roll damping	365. Kgmsec/rad
rear roll damping	350. Kgmsec/rad
static camber on front and rear wheels	0.
front wheels camber variation per unit roll angle	0.92
rear wheels camber variation per unit roll angle	0.
front roll steering	0.
rear roll steering	0.

Equation for the side force F for the tire:

$$F = \frac{3}{2}\ \mu\ \frac{a}{a_m}\left[1 - \frac{1}{3}\left(\frac{a}{a_m}\right)^2\right] P$$

where:

μ = limiting coefficient of friction = $\mu_o\left(1 - \frac{P}{22_m}\right)$

μ_o = coefficient of friction for P = O or $P_m = \infty$

a = slip angle.

a_m = slip angle which, for P = constant, gives the max. lateral force.

P = vertical load on the tire.

P_m = vertical load which, for a = constant, gives the max. lateral force.

for the front tires : $\mu = 0.9$ (for static load)
$a_m = 9°$
$P_m = 500$ Kg

for the rear tires : $\mu = 0.9$ (for static load)
$a_m = 9°$
$P_m = 500$ Kg

front axle lateral force variation per unit camber angle	700. Kg/rad
rear axle lateral force variation per unit camber angle	650. Kg/rad

Equation for the rolling resistance R of the vehicle:

$$R = P(a + b\,u^2)\ (Kg)$$

P = vehicle weight (Kg)

a = 0.01075

$b = 6.5 \cdot 10^{-6}$ sec^2/m^2

u = vehicle forward speed (m/sec)

max. vehicle cross sectional area	1.7 m^2
aerodynamic resistance coefficent	0.414
front aerodynamic lift coefficent	0.218
rear aerodynamic lift coefficient	0.019

Starting from the above data, the following variations were considered:

Case 1 and 2 – Degree of understeering.

This was varied by changing the value of a_m (preceding page)

This value was reduced by 20% for the front and rear axle successively, following the scheme below:

	a_m	
	front	rear
Case 1 – Understeering increase	10.8	9
Case 2 – Understeering decrease	9.	10.8

Case 3 – Roll steering.

The following factor was introducted for the rear axle, reducing stability:

$$e = \frac{\text{Rear roll steering angle}}{\text{Roll angle}} = 0.15$$

It must be remembered that front and rear roll oversteering effects are practically identical.

Case 4 – Simultaneous increase in weight and radius of inertia.

weight increase : 20%

rad. of inertia increase : 10%

These increases could be found in vehicles modified to satisfy passive safety requirements.

We point out that the weight increase influences directly the limiting friction coefficient, according to the formulas shown on the preceding page.

Figure 1 compares the steady state behavior of the different solutions mentioned above with the American ESV limits.

Figure 2 shows a similar comparison for transient state, high speed behavior.

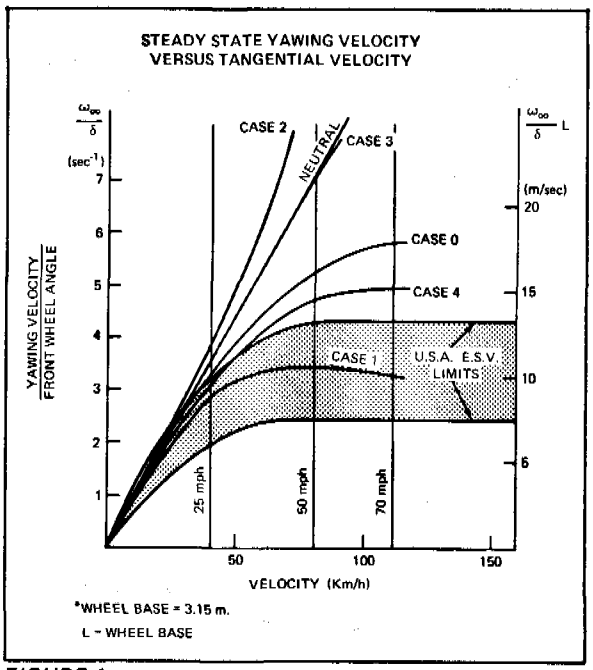

FIGURE 1

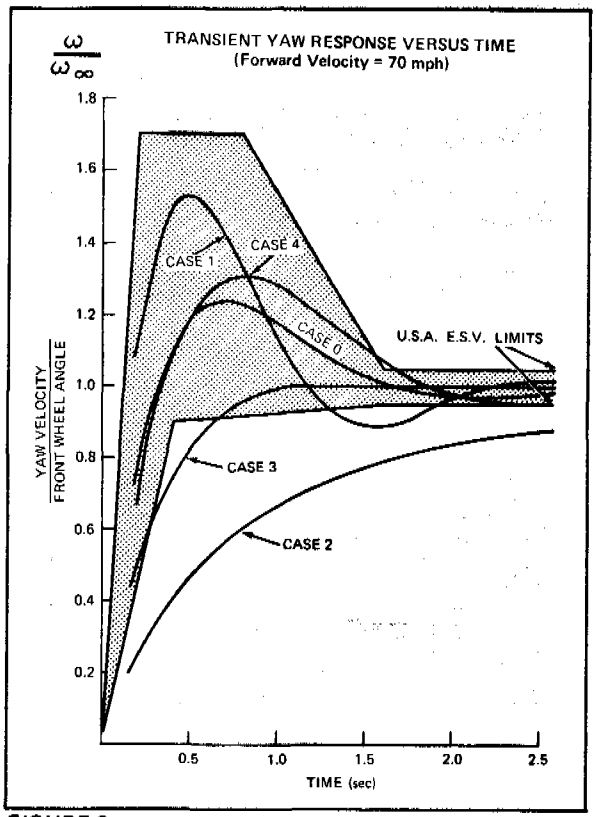

FIGURE 2

It can be seen that only the vehicle with increased understeering (case 1) is within the ESV limits for the steady state test. With the exception of case 2 vehicle

(oversteering), all cars are substantially within the ESV limits for transient state yaw.

Change of trajectory on a straight road

The vehicle travels at 70 mph on a straight road having 3 lanes, each 3 m. wide. The initial trajectory of the vehicle is along the centerline of the central lane.

At a point which is halfway of the braking distance required with 0.4 g deceleration from an obstacle using up the central and right hand lanes, the driver decides to change his trajectory, and to follow the centerline of the left hand lane, as shown in Figure 3 and in the following ones.

Figures 3, 4, 5, 6, 7 show the trajectories, the lateral acceleration and front wheels steering angles diagrams for vehicle case 0, 1, 2, 3, 4 respectively.

By examining the above named figures, and the following table, it can be observed that:

- All other factors being equal, a reduction of the degree of understeering (starting from the base vehicle), no matter how it is obtained, reduces the stability of the vehicle. For vehicles case 2 (oversteering) and case 3 (almost neutral), the trajectory diverges.

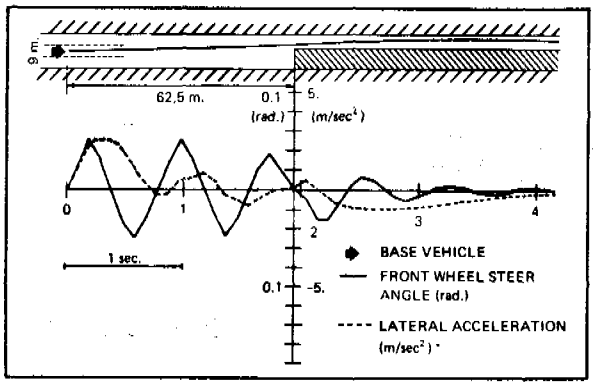

FIGURE 3

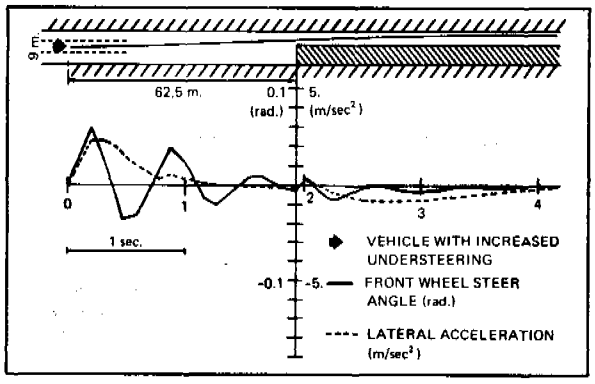

FIGURE 4

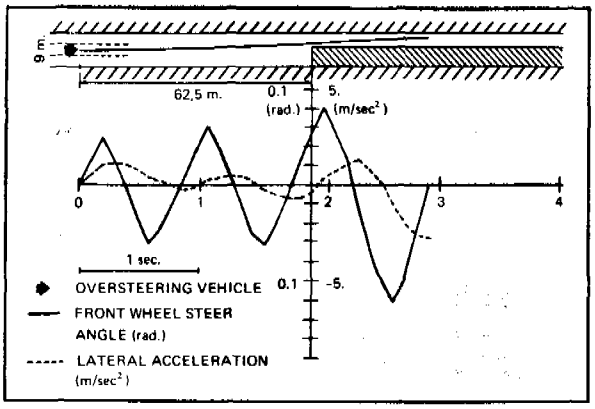

FIGURE 5

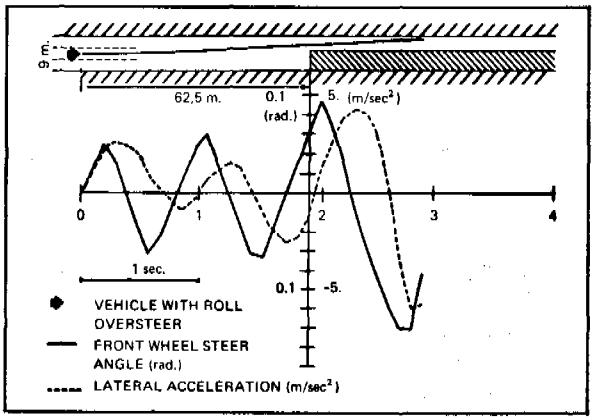

FIGURE 6

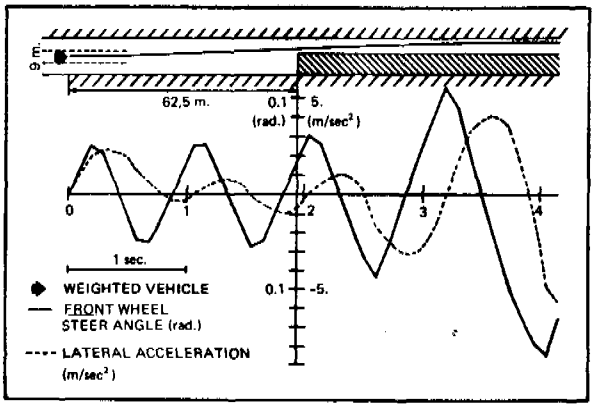

FIGURE 7

On the other hand, an increase in the degree of understeering (case 1) improves vehicle stability, at the cost of decreasing handling quality, as can be observed from the maximum steering angles values measured during the maneuver.

The weighted vehicle too showed an unstable behavior, even if it was more understeering than the base vehicle.

CASE	δ max	Δ° (18) max	Δ° (28) max	Marg.	
0 BASE VEHICLE	0.0506	52.2	81.2	0.39	CONVERGES
1 VEHICLE WITH INCREASED UNDERSTEERING	0.0600	61.9	96.3	0.33	CONVERGES
2 OVERSTEERING VEHICLE	0.1212	125.1	194.5	< 0	DIVERGES*
3 VEHICLE WITH ROLL OVERSTEER	0.1416	146.1	227.0	< 0	DIVERGES*
4 **WEIGHTED VEHICLE**	0.1691	174.5	271.5	< 0	DIVERGES*

where: δ_{max} = max. front wheels steering angle, in radians.
Δ°_{max} (18) = max. steering wheel rotation angle, for a steering wheel/front wheels ratio = 18.
Δ°_{max} (28) = max. steering wheel rotation angle, for a steering wheel/front wheels ratio = 28.
Marg. = minimum distance of the vehicle from the obstacle (m).

*For all three cases of divergence, the vehicle leaves the road, after complete loss of adhesion.

This was due to the worsening response time of the vehicle, caused by the increased moment of inertia radius with respect to the yaw axis, and by tires which had become undersized as a consequence of the weight increase.
Obviously, this last factor could easily be corrected by fitting wider section tires.

- Taking into consideration only understeering vehicles, it can be observed that there is a vehicle which shows a good behavior, but does not comply with the limits imposed (case 0). The only vehicle which complies with the American ESV proposal (case 1) also shows a good behavior, but is slightly less good in handling.

STUDY OF AN UNDULATED SURFACE FOR ROAD-HOLDING TESTS

A fundamental characteristic of the vehicle, in order to judge its active safety quality, is its behavior on a rough surface. Such behavior involves not only considerations on comfort, but especially on road-holding.

Indeed, even today many busy roads are far from that condition of maintenance, use, and weather protection, which would allow us to disregard the effect of surface roughness on adhesion. We intend to talk about the disturbances caused both by isolated obstacles (such as expansion joins and resurfacing connections) and by casual surface irregularities, which may be represented as a continuous "Power Spectrum," and are characteristic of every type of surface, reaching particular intensity on "pave" and non-asphalted roads.

It is well known that many Research Institutions [A] have undertaken work on the "Power Spectrum" of roads, motorways and landing strips (Figure 8.)

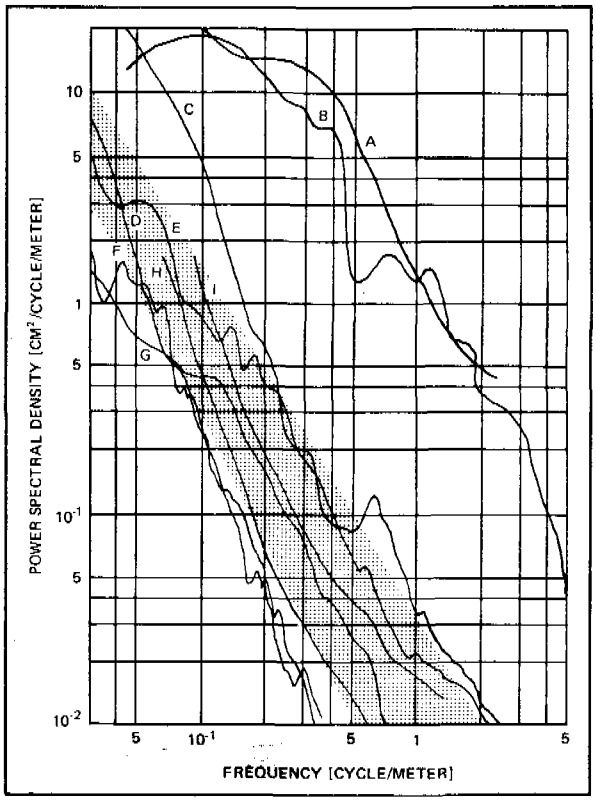

FIGURE 8

Description of the types of roads of Fig. 8

PROFILE	TYPE OF PAVING	SOURCE
A	M.I.R.A. Pave – 1 Section	M.I.R.A. Report 1964/9
B	Endurance test surface	I. Kaneshige S.A.E. Paper 690111
C	Rough French Road	A. Pasquet S.I.A. 10/70
D	Good French Road	A. Pasquet S.I.A. 10/70
E	Medium sized stone slabs	Mitschke Dynamik der Kraftf.
F	Asphalt road, very good	Mitschke Dynamik der Kraftf.
G	Concrete road, reasonable	Mitschke Dynamik der Kraftf.
H	U.S.A. highway, very good	M.I.R.A. Report 1964/9
I	U.S.A. highway, fairly good	M.I.R.A. Report 1964/9

Some authors [B] have reproduced chosen "Power Spectra," actually achieving randomly undulated surfaces.

We believe that, theoretically, such methods of reproduction, or simplified methods (like the one adopted by ourselves [C], can solve very well the problem of simulating profiles of desired statistical and spectral characteristics.

As far as road-holding tests are concerned (and differently from durability tests for mechanical parts), it seems better to use moderately rough surfaces, as they are the most similar to average usage conditions. From an installation viewpoint, this means that the methods [B] and [C] would require a precision incompatible with normal building methods (as the amplitude of the asperities would be about 1/10 that of a durability test pave.)

On the other hand, building precision is required by the practical necessity of condensing in the shortest possible length (a few hundred meters, at the most) the statistical and spectral characteristics of real or chosen standard roads.

All that was said up to now can be summed up in the following conditions, which impose limitations to the practical possibilities for the choice of the type of surface and test:

C1 – Moderately rough surface.

C2 – Admissible errors in the profile amplitudes (of the order of a few millimeters).

C3 – Profile Power Spectrum, representative of real roads, or at least such that the Power Spectral Density decreases as the frequency increases (i.e., as the wave lengths decrease.)

C4 – Power Spectrum extended over a frequency range such that it covers, at the testing speed, at least the frequency interval pertinent to the suspension (0.5 20 Hz), or at least the most important frequency band as far as tire/ground contact is concerned (9 ÷ 18 Hz.)

C5 – The shortest possible test length, compatible with the need of having at least 3 complete waves of the lowest frequency component.

C6 – Realistic correlation between the profile amplitudes which excite simultaneously the four wheels.

C7 – "Normal" distribution of the exciting amplitudes.

C8 – A suitable test for evaluating an average vehicle behavior during the experiment.

C9 – Moderate test speed, for obvious safety reasons.

The conditions C1-C2-C5-C9 combined, imply the necessity of excluding continuously undulated profiles, such as those generated by sinusoidal, superimposed waves [C]

A profile thus defined may indeed be represented by an equation of the type:

$$y(x) = \sum_{1}^{n} {}_{k}\, y_k \quad \sin\left(2\pi k \frac{x}{L} + \varphi_k\right)$$

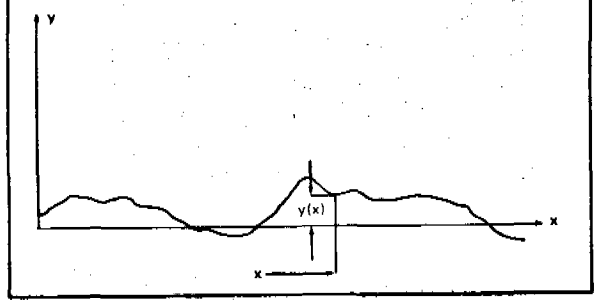

where:

y_k = amplitude of the k^{th} component of the development.

φ_k = phase of k^{th} component of the development.

L = period of the profile function, equal or greater than the total development of the profile.

The phase φ_k is really the casual element of the development. The amplitude y_k has a well-defined value, with respect to the Power Spectral Density S_y of the profile to be reproduced, and to the amplitude of the frequency band Δfk. The Power Spectrum content of this frequency band is totally debited to the sinusoidal with frequency f_k and amplitude y_k.

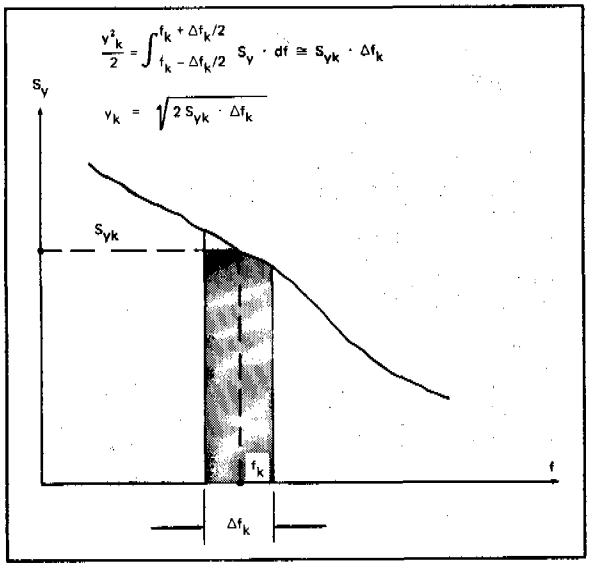

If, for example, in connection with the value f_k = 0.5 (cycles/m) we assume a value $s_{yk} = 2 \times 10^{-2}$ (cm^2/cycles/m) and a very large band amplitude, $\Delta f_k = f_k = 1$ (cycles/m), we obtain the following amplitude of the k^{th} component:

$$y_k = \sqrt{4.10^{-2}} = 0.20 \text{ [cm]}$$

This shows the practical impossibility to build, with normal methods and materials, wave lengths equal to or shorter than 2 metres; on the other hand, such length is equivalent to an exciting frequency of 10 Hz, intermediate in the range of frequencies with which we are concerned, even at the considerable test velocity of 20 m/sec (45 mph.)

As a consequence we must resort to asperities which, even though exciting frequencies higher than 10 Hz, are sufficiently high. Such are impulsive type obstacles, which we will represent with a rectangular profile, characterized by a much smaller base than the shortest wave length with which we are concerned.

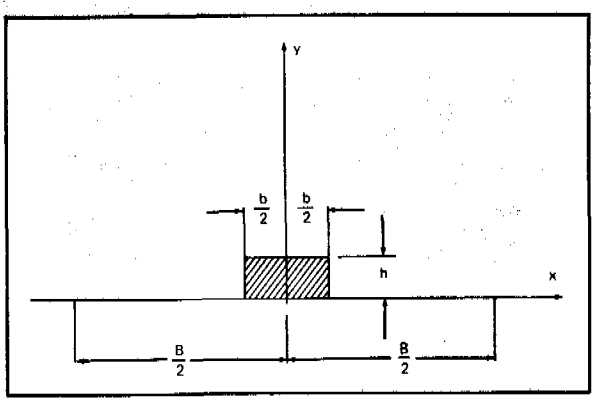

Considering one of these obstacles, assumed periodic with period = B, it can be described mathematically using a Fourier series:

$$y(x) = \frac{a_0}{2} + \sum_1^\infty {}_k \left(a_k \cos 2\pi k \frac{x}{B} + b_k \sin 2\pi k \frac{x}{B} \right)$$

$$a_0 = \frac{2}{B} \int_{-B/2}^{B/2} y(x)dx = \frac{2bh}{B}$$

$$a_k = \frac{2}{B} \int_{-B/2}^{B/2} y(x)\cos\left(2\pi k \frac{x}{B}\right) dx = \frac{2h}{\pi k} \sin\left(\frac{\pi kb}{B}\right)$$

$$b_k = \frac{2}{B} \int_{-B/2}^{B/2} y(x)\sin\left(2\pi k \frac{x}{B}\right) dx = 0.$$

The amplitude y_k of the k^{th} component of the series development becomes then:

$$y_k = \frac{2h}{\pi k} \left| \sin \frac{\pi kb}{B} \right|$$

For $\pi kb << B$, the above expression becomes:

$$y_k = y_{ko} = \frac{2h}{\pi k} \frac{\pi kb}{B} = \frac{2hb}{B}$$

that is, the amplitude of the components remain constant, independently from k.

Furthermore, the general expression for y_k becomes = 0 for the first time when $\frac{kb}{B} = 1$, i.e. $k^* = \frac{B}{b}$.

We want to find the trend of the amplitudes y_k for $1 < k < k^*$.

$$\frac{dy_k}{dk} = \frac{d}{dk}\left[y_{ko} \frac{B}{b} \frac{1}{\pi k} \sin \frac{\pi kb}{B} \right] =$$